Electronic Supporting Information

for

A Tutorial for Understanding Chemical Reactivity Through The Valence Bond Approach

Dandamudi Usharani,[a] Wenzhen Lai,[b] Chunsen Li,[c] Hui Chen,[d]

David Danovich[a] and Sason Shaik*[a]

[a] Institute of Chemistry and The Lise Meitner-Minerva Center for Computational Quantum Chemistry, The Hebrew University of Jerusalem, 91904, Jerusalem, Israel

[b] Department of Chemistry, Renmin University of China, Beijing, 100872, China

[c] State Key Laboratory of Structural Chemistry, Fujian Institute of Research on the Structure of Matter, Chinese Academy of Sciences, Fuzhou, Fujian 350002, China; Fujian Provincial Key Laboratory of Theoretical and Computational Chemistry, Xiamen, Fujian 361005, China

[d] Beijing National Laboratory for Molecular Sciences (BNLMS), CAS Key Laboratory of Photochemistry, Institute of Chemistry, Chinese Academy of Sciences, Beijing, 100190, China

Table of Contents:

Additional References:

1. **Other reviews on VB and Chemical reactivity**. The following reviews, as well as those mentioned in the text, include applications to a great variety of reactions: (a) S.S. Shaik and P. C. Hiberty, *Curve Crossing Diagrams as General Models for Chemical Reactivity and Structure in* Theoretical Concepts for Chemical Bonding, Invited Review, 1991, **4**, 324-378. (b) S. Shaik, *Pure Appl. Chem*., 1991, **63**, 195. (c) S. Shaik, in New Theoretical Concepts for Understanding Organic Reactions, ed. J. Bertran, G.I. Csizmadia, Kluwer Publ., Dordrecht, Holland, 1989. [this review derives a semi-empirical Hückel type VB approach for conceptual understanding] (d) S. Shaik, *J. Mol. Liq.*, 1994, **61**, 49. (e) S. Shaik and A. C. Reddy, *J. Chem. Soc., Faraday Trans*., 1994, **90**, 1631. (f) S. Shaik, The Valence Bond Curve Crossing Model for Chemical Reactivity: An Interface between Computational Chemistry, Theory and Experiment in Encyclopedia of Computational Chemistry, 1998, **5**, 3143. P. v. R. Schleyer, H. F. Schaefer, P. R. Schreiner, Eds., Wiley & Sons. (g) S. Shaik, P. C. Hiberty, A Valence Bond Diagram Approach - A Paradigm for Chemical Reactivity, in: Theory and Applications of Computational Chemistry: The First 40 Years, ed. C.E. Dykstra, G. Frenking, K. S. Kim, G. E. Scuseria, Elsevier, Amsterdam, 2005 Ch. 23, pp 635. (h) S.S. Shaik, *Acta Chem. Scand.* 1990, **44**, 205.

2. **Quantitative VB studies of chemical reactions:** (a) G. Sini, S. Shaik and P. C. Hiberty, *J. Chem. Soc., Perkin Trans*., 1992, **2**, 1019. (b) J. M. Galbraith, P. R. Schreiner, N. Harris, W. Wu, A. Wittkopp and S. Shaik, *Chem - Eur. J*., 2000, **6**, 1446. (c) W. Wu, W. H. Saunders and S. Shaik, *Can. J. Chem*., 2005, **83**, 1649. (d) P. Su, F. Ying, W. Wu, P. C. Hiberty and S. Shaik, *Chem. Phys .Chem*., 2007, **8**, 2603. (e) P. Su, L. Song, W. Wu, S. Shaik and P. C. Hiberty, *J. Phys. Chem. A*, 2008, **112**, 2988. (f) https://wiki.lct.jussieu.fr/workshop/index.php/ VB_workshop _in_Paris

3. **Various reactions**:
   S_N2 reactions:(a) A. Pross and S. Shaik, *J. Am. Chem. Soc.,* 1981*,* **103***,* 3702. (b) S. S. Shaik, *Nouv. J. Chim*., 1982, **6**, 159. (c) S. Shaik, *J. Am. Chem. Soc.,* 1983*,* **105***,* 4359. (d) S. Shaik, *J. Am. Chem. Soc.,* 1984*,* **106***,* 1227 (this develops VBSCD with solvent effect). **S_NV, vinylic nucleophilic substitution reactions:** (e) D. Cohen, R. Bar, S.S. Shaik, *J. Am. Chem. Soc.,* 1986*,* **108***,* 231. (f) **Nucleophilic cleavage of esters:** E. Buncel, S.S. Shaik, I.-H. Um, S. Wolfe, *J. Am. Chem. Soc.,* 1988*,* **110***,* 1275. (g) **Anion-Cation Recombinations**: S.S. Shaik, *J. Org. Chem*. 1987, **52**, 1563. (h) **Bonded Electron transfer**: L. Eberson, S.S. Shaik, *J. Am. Chem. Soc.,* 1990*,* **112***,* 4484. (i) **Reactions of anion radicals with alkyl halides – entangled reactivity:** G.N. sastry, S. Shaik, *J. Phys. Chem.* 1996, **100**, 12241. (j) **cyclization reactions:** J.M. Galbraith, P.R. Schreiner, N. Harris, W. Wu, A. Wittkopp, *Chem. Eur. J.* 2000, **6**, 1446. (k) **Bond activation by**

Pd catalysts: S. Kozuch, S. Shaik, A. Jutand, C. Amatore, *Chem. Eur. J.* 2004, **10**, 3072. (l) **Bond heterolysis in solution:** P. Su, L. Song, W. Wu, S. Shaik, P.C. Hiberty, *J. Phys. Chem. A*, 2008**,** **112**, 2988. (m) **Elimination reactions:** W. Wu, S. Shaik, W.H. Suanders, *J. Org. Chem.* 2010, **75**, 3722. (n) **Cycloadditions:** R. Meir, H. Chen, W. Lai, S. Shaik, *ChemPhysChem.* 2010, **11**, 301.

4. **Predictions of stereoselectivity and regioselectivity using VB theory:** (a) L. Eberson, R. González-Luque, M. Merchán, F. Radner, B. O. Roos, S. Shaik, *J. Chem. Soc., Perkin Trans*. 1997*,* **2**, 463. (b) S. S. Shaik, E. Canadell, *J. Am. Chem. Soc.* 1990, **112**, 1446. (c) S. S. Shaik, J. P. Dinnocenzo, *J. Org. Chem.* 1990, **55**, 3434. (d) See also Refs. 14 and 29 in the text. Ref. 29 especially includes problem sets and answers. It is a good source for tutoring.

5. **Some Computational VB Methods:**
(a) GVB: W. A. Goddard, *Phys. Rev.* 1967, **157**, 81*.* (b) Spin Coupled VB theory: P. B. Kardakov, J. Gerrat, D. L. Cooper, M. Raimondi, *Theor. Chim. Acta* 1995*,* **90***,* 51**.** (c) Usage of Young Tableaux: G. A. Gallup, J. M. Norbeck, *Chem. Phys. Lett.* 1973, **21**, 495. (d) XMVB: L. Song, Y. Mo, Q. Zhang, W. Wu, *J. Comput. Chem.* 2005, **26**, 514; 2009, **30**, 399. (e) BOVB: P. C. Hiberty in *Modern electronic Structure Theory and Applications in Organic Chemistry.* Ed. E. R. Davidson, World Scientific, River Ridgde, New York, **1997**, pp. 289-367*.* (f) TURTLE: J. Verbeek, J. H. Lagenberg, C. P. Byrman and J. H. van Lenthe, TURTLE and Ab Inito VB/VBSCF Program (1988-2000). At present the program is installed in GAMESS-UK. (g) CASVB: Written by D. L. Copper and incorporated in MOLPRO.

Part Ia. HAT Reactions of Cpd I with Different Alkanes

Table S1 collects the raw data for calculating barriers for the HAT reactions of Cpd I with the alkanes **1-15** in Figure 5 in the text. These are the requisite data for reproducing Figure 7 in the paper. This and other tables are useful for self-tutoring.

Table S1. DFT calculated $BDE_{FeO\text{-}H}$, $|RE_{FeO}|$, $D_{FeO\text{-}H}$, $BDE_{H\text{-}Y}$, $|RE_{Y\bullet}|$, $D_{H\text{-}Y}$, and barrier for hydroxylation.[a]

Oxidant	$BDE_{FeO\text{-}H}$	$\|RE_{FeO}\|$	$D_{FeO\text{-}H}$			
CpdI	89.28	14.94	104.22			
Substrate	$BDE_{H\text{-}Y}$	$\|RE_{Y\bullet}\|$	$D_{H\text{-}Y}$	$\Delta E^{\ddagger}_{HS}$[b]	$\Delta E^{\ddagger}_{LS}$[b]	$\Delta E^{\ddagger}_{VB}$[c]
Methane (**1**)	101.62	6.79	108.41	22.91	22.34	18.27
Ethane (**2**)	96.87	7.00	103.87	17.41	15.30	15.54
i-Propane (**3**)	93.03	7.21	100.24	15.80	13.85	13.36
n-Propane (**4**)	97.49	6.87	104.36	17.48	15.19	15.84
Propene (**5**)	82.80	16.69	99.49	12.95	12.82	12.91
(**6**) trans-methyl phenylcyclopropane	93.62	8.30	101.92	14.53	13.13	14.37
(**7**) trans-i-propyl phenylcyclopropane	86.60	8.60	95.20	13.46	12.27	10.34
N,N-DMA (**8**)	86.08	7.94	94.02	5.54	4.99	9.63
Toluene (**9**)	85.80	12.27	98.07	12.43	12.05	12.06
Phenylethane (**10**)	82.45	18.38	100.83	12.55	11.47	13.72
Camphor (**11**)	93.89	7.61	101.50	14.51	15.88	14.12
p-CN-DMA (**12**)	85.98	9.09	95.07	10.10	9.47	10.26
p-NO_2-DMA (**13**)	85.94	9.76	95.70	10.82	10.31	10.64
p-Cl-DMA (**14**)	85.42	8.57	93.99	7.17	6.49	9.61
Cyclohexane (**15**)	93.05	7.15	100.20	15.57	14.82	13.34

[a]All data are the values at the UB3LYP/B2 (B2 involves LACV3P+* for iron and 6-311+G* for the rest) level with ZPE correction. $BDE_{FeO\text{-}H}$ and RE_{FeO} are the average of the HS and LS values.

[b] $\Delta E^{\ddagger}_{HS}$ and $\Delta E^{\ddagger}_{LS}$ are the respectively, corresponding barriers for the quartet and doublet spin states of Cpd I. $\Delta E^{\ddagger}_{av(DFT)}$= ½ ($\Delta E^{\ddagger}_{HS}$+$\Delta E^{\ddagger}_{LS}$)

[c] $\Delta E^{\ddagger}_{VB} = 0.6 D_{H\text{-}Y}$ - 46.78 (kcal/mol); using equation 7.

Part Ib. Arene Activation by Cpd I

For the sake of self-tutoring we are giving a detailed explanation of how to gauge *B* due to mixing of a charge transfer state. For further details see ref. 27 cited in the paper. The following VBCMD shows that the CT state should be close to the two principal curves, and hence it will mix into the two principal curves, thus affecting *B*.

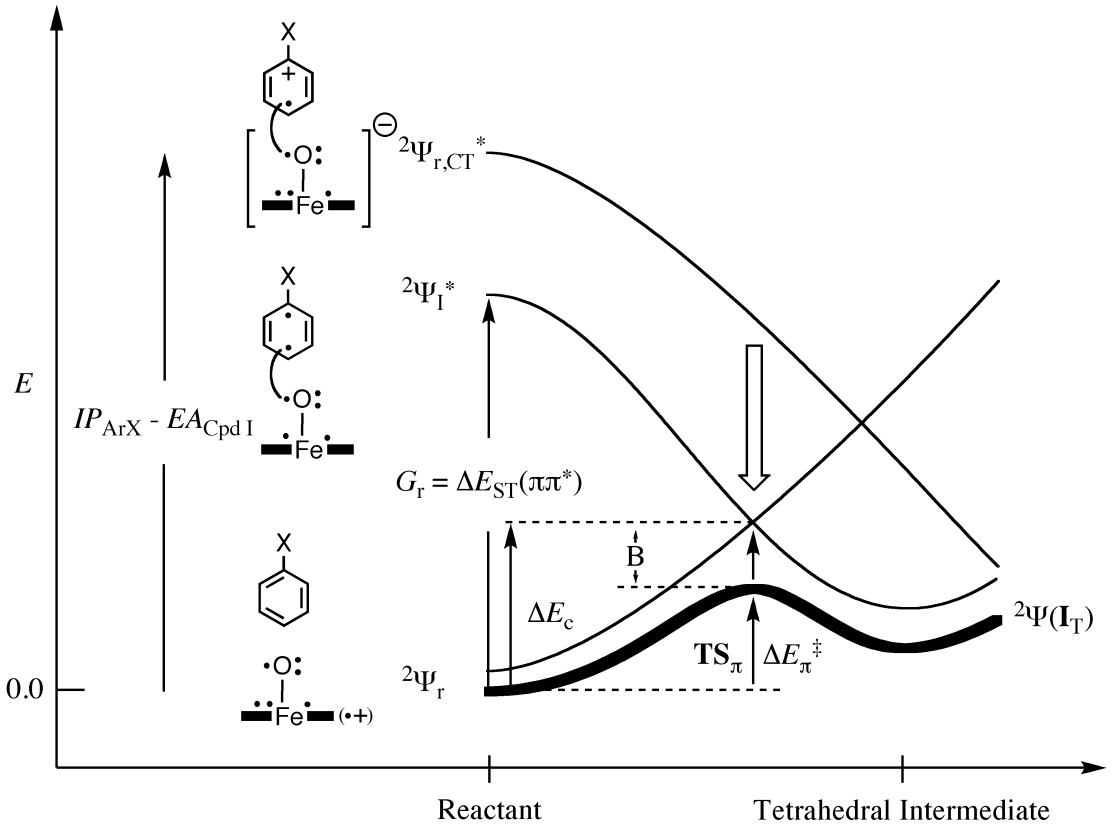

Figure S1. VBCMD for the π-activation step of arenes, showing the three state curves and the key quantities that determines the barrier.

As usual, the height of the crossing point can be expressed as a fraction of the singlet-triplet promotion energy at the reactant side leading to eq. S.1:

$$\Delta E_p^\ddagger = f\Delta E_{ST} - B \qquad \text{(S.1)}$$

Here, f =0.3, while *B* reflects the mixing in the charge transfer state, which lies above the reactant state by the CT energy:

$$\Delta E_{CT}\,(^2\Psi_r \rightarrow {}^2\Psi_{r,CT}{}^*) = IP_{ArX} - EA_{Cpd\ I} \qquad \text{(S.2)}$$

where IP_{ArX} is the ionization potential of the substituted arene, while $EA_{Cpd\ I}$ is the electron affinity of Cpd I.

Using perturbation theory, the mixing of the CT state into the TS will be inversely proportional to the energy gap between the charge transfer $\Psi_{r,CT}$* and the crossing point in Figure S1, and proportional to the matrix element that couples the states. Since the energy gap of the crossing point is proportional to IP_{ArX}– EA_{CpdI}, and since the matrix element for coupling these states is gauged by the odd electron density on the carbon site in the triplet $\pi\pi$* promoted state where O---C bond is made, we can use the following simple expression for B_X for a given substituent X, relative to B_H for the unsubstituted benzene:

$$B_X = B_H \{[\rho_X(IP_H - EA_{Cpd\ I})]/[\rho_H(IP_X - EA_{Cpd\ I})]\} \quad \text{(S.3a)}$$

$$B_H = f\Delta E_{ST,H} - \Delta E_p^{\ddagger}(DFT)_H \ ; \ f = 0.3 \quad \text{(S.3b)}$$

$$B_H = 14.5 \text{ kcal/mol} \quad \text{(S.3c)}$$

Here ρ_X and ρ_H are, respectively, the spin densities at the sites of attack of the X-substituted arene vs. benzene, in the corresponding $\pi\pi$* triplet states. As shown in eq. S.3b, the B_H value for benzene is extracted from the difference between the VB height of the crossing point and the corresponding DFT barrier, leading to B_H=14.5 kcal/mol (eq. S.3c), which serves to calculate all other B_X values. The so calculated B values and the corresponding VB barriers are collected in Table S2.

Part Ic. Bond Activation of olefins and arenes by Cpd I

The modeling of olefin and arene bond activation follows the same outline as arene activation alone. Table S2 shows the corresponding data using now the activation of benzene by Cpd I (SCH_3) as a standard for gauging the relative *B* values for all other substrates. These are the requisite data for reproducing Figure 8 and 9b in the paper.

Table S2. Reactivity Factors, and VB Estimated B_X Values and Barriers for olefin activation and the *para* Position Attacks by Cpd I on ArX Molecules. The reaction of **benzene** with **Cpd I (SCH_3)** serves as a standard. f = 0.3. MUE=1.13 kcal/mol. Note EA_{CpdI} = 64.9 kcal.mol^{-1} B_H= $0.3\Delta E_{ST} - \Delta E^{\ddagger}_{DFT}$ = 14.5 kcal/mol.

Substrate	IP^{NIST}	$\Delta E_{ST}{}^{V\,a}$	ρ_X	$B_{X,(VB)}{}^{b}$	$\Delta E^{\ddagger}_{VB}{}^{c}$	$\Delta E^{\ddagger}_{DFT}{}^{d}$
ethene	242.1	100.6	1.14	16.1	14.1	14.3[d]
propene	229.9	99.9	1.20	18.2	11.8	12.6[d]
1-butene	226.7	99.8	1.20	18.5	11.4	*11.1*[d]
trans-2-butene	215.0	99.0	1.05	17.5	12.2	10.0[d]
1,4-CHD[e]	203.3	98.1	1.06	19.1	10.3	*11.9*[d]
benzene (Cpd I(SH))	213.1	102.2	0.86	14.5	16.2	15.8[d]
C_6F_6	232.5	68.5	0.73	10.9	9.7	8.9[f]
C_6Cl_6	213.6	87.3	0.69	11.6	14.6	15.0[f]
ArX activation	IP^{NIST}	$\Delta E_{ST}{}^{V\,a}$	ρ_X	$B_{X,(VB)}{}^{b}$	$\Delta E^{\ddagger}_{VB}{}^{c}$	$\Delta E^{\ddagger}_{DFT}{}^{d}$
Benzene (Cpd I(SCH_3))	213.1	102.2	0.86	14.5	16.2	16.2[g]
Cl	209.4	97.3	0.80	13.8	15.4	15.3[g]
F	214.0	101.9	0.83	13.9	16.7	15.2[g]
CN	225.3	89.3	0.75	11.7	15.1	14.9[g]
NO_2	232.0	87.1	0.76	11.4	14.8	14.2[g]
NMe_2	174.1	89.4	0.76	17.4	9.4	9.6[g]
OMe	193.7	97.6	0.82	15.9	13.4	13.2[g]
NH_2	185.4	91.5	0.76	15.7	11.7	11.0[g]
CH_3	205.0	99.0	0.89	15.9	13.8	15.0[g]
SMe	187.7	95.9	0.75	15.2	13.5	12.6[g]
N-acetyl	195.1	91.1	0.75	14.4	13.0	13.6[g]
1,2-difluoro-benzene[i]	217.9	102.6	0.87	14.2	16.6	16.6[h]
2-fluoro-aniline	188.6	88.6	0.64	12.9	13.7	11.7[g]
2,6-difluoro-aniline	197.9	91.6	0.84	15.8	11.7	12.0[h]
2,3,6-trifluoro-aniline	195.8[a]	90.6	0.75	14.3	12.9	11.8[h]

[a]Calculated values (B3PW91/6-311++G**). [b]$B_{X\,(VB)} = B_H\,\{[\rho_X(IP_H - EA_{Cpd\,I})]/[\rho_H(IP_X - EA_{Cpd\,I})]\}$ [c]$\Delta E^{\ddagger}_{VB}$ using equation S.1. [d]Activation energies correspond to radical-cationic transition states at the doublet electronic state published by Kumar, D. et al *JACS* **2010**, *132*, 7656-7667. Numbers in italics correspond to radical-cationic transition states at the quartet electronic state. [e]CHD stands for cyclohexadiene. [f]RI-PBE/TZVPP barriers (TS energies relative to the separate reactant) taken from *Biochemistry* **2007**, *46*, 5924-5940. [g]Obtained from *J. Chem. Theory Comput.* **2011**, *7*, 327-339. [h]Obtained from *Org. Biomol. Chem.* **2004**, *2*, 2998-3005. [i]positions 3,6.

Part II Hydrogen atom transfer (A-Y)

(a) Identity and Nonidentity reactions of (Figure 10a,b) X• + H-Y → X-H + •Y

Table S3. CCSD(T)/CBS bond dissociation energies (BDE), reorganization energies (RE_Y), and bond strength (*D*) of H-Y bonds.[a]

H-Y	BDE CBS[b]	$RE_{Y\bullet}$	*D* CBS[b]
H	103.17	0.00	103.17
F	135.06	0.00	135.06
Cl	102.54	0.00	102.54
Br	88.70	0.00	88.70
I	77.00	0.00	77.00
CH_3	103.16	6.85	110.01
SiH_3	90.10	0.15	90.25
GeH_3	82.74	0.11	82.85
SnH_3	74.10	0.18	74.28
PbH_3	64.94	0.23	65.17
OH	116.95	0.02	116.97
SH	89.47	0.01	89.48
NH_2	105.28	0.08	105.36
C_2H	132.87	0.08	132.95
CH_2CN	95.71	10.74	106.45

[a]All data are in kcal/mol, taken from the ESI of *Angew. Chem. Int. Ed*. **2012**, *51*, 5556. (Ref.17 in the text). [b]CBS values with ZPE correction. CBS = complete basis set limit.

Table S4. DFT calculated BDE_{FeO-H}, D_{FeO-H}, BDE_{H-Y}, RE_Y, D_{H-Y} and barriers for hydroxylation by Cpd I.[a]

Substrate (H-Y)	BDE_{H-Y}	RE_Y	D_{H-Y}	$\Delta E^{\ddagger}_{av}$	$\Delta E^{\ddagger}_{VB}(1)$[b]	$\Delta E^{\ddagger}_{VB}(9)$[b,c]
Methane (**1**)	101.62	6.79	108.41	22.63	22.23	22.59
Ethane (**2**)	96.87	7.00	103.87	16.36	19.68	19.82
i-Propane (**3**)	93.03	7.21	100.24	14.83	17.64	17.67
n-Propane (**4**)	97.49	6.87	104.36	16.34	19.99	20.15
Propene (**5**)	82.80	16.69	99.49	12.89	14.85	14.96
(**6**) *trans*-methyl phenylcyclopropane	93.62	8.30	101.92	13.83	18.29	18.33
(**7**) *trans*-*i*-propyl-phenylcyclopropane	86.60	8.60	95.20	12.87	14.52	14.53
N,*N*-DMA (**8**)	86.08	7.94	94.02	5.27	14.03	14.06
Toluene (**9**)	85.80	12.27	98.07	12.24	15.18	15.21
Phenylethane (**10**)	82.45	18.38	100.83	12.01	15.17	15.28
Camphor (**11**)	93.89	7.61	101.50	15.20	18.23	18.28
p-CN-DMA (**12**)	85.98	9.09	95.07	9.79	14.32	14.35
p-NO_2-DMA (**13**)	85.94	9.76	95.70	10.57	14.5	14.53
p-Cl-DMA (**14**)	85.42	8.57	93.99	6.83	13.86	13.9
Cyclohexane (**15**)	93.05	7.15	100.20	15.67	17.63	17.66
Oxidant CpdI (L_{ax})	BDE_{FeO-H}		D_{FeO-H}			
SH	89.28		104.22			
OAc(**16**)	89.09		99.88			
Cl(**17**)	87.62		96.43			
CF_3SO_3(**18**)	81.38		94.07			
H-Y+X	BDE_{H-Y}	RE_Y	D_{H-Y}	$\Delta E^{\ddagger}_{av}$	$\Delta E^{\ddagger}_{VB}(1)$[b]	$\Delta E^{\ddagger}_{VB}(9)$[b,c]
Cyclohexane with **16**	93.05	7.15	100.20	17.07	16.47	16.51
Cyclohexane with **17**	93.05	7.15	100.20	17.29	16.54	16.61
Cyclohexane with **18**	93.05	7.15	100.20	18.62	20.51	20.86

[a]The data are the values with ZPE correction at the LACV3P+*//LACVP, All data are taken from the SI of *Angew. Chem. Int. Ed*. **2012**, *51*, 5556 (ref 17 in the text).

[b] The equation numbers 1 and 9 refer to their numbers in the text

$\Delta E^{\ddagger}_{VB}(1) = 0.3G_0 + 0.5\Delta E_{rp}$ - B; B = 0.25(BDE_{H-Y} + BDE_{H-X}).

[c]$\Delta E^{\ddagger}_{VB}(9) = \Delta E^{\ddagger}_{VB}(1) + 0.5(\Delta E_{rp})^2/G_0$.

The calculated reaction energies (ΔE_{rp}) and barriers ($\Delta E^{\ddagger}_{calc}$) and estimated VB Barriers.

Table S5. The CCSD(T)/CBS[a] calculated $\Delta E^{\ddagger}_{calc}$ and ΔE_{rp} values, along with valence bond barriers $\Delta E^{\ddagger}_{VB}(1)$ and $\Delta E^{\ddagger}_{VB}(9)$ for X• + H-Y→ X-H + •Y reactions

X• + H-Y→ X-H + •Y	$\Delta E^{\ddagger}_{calc}$ [a]	ΔE_{rp} [b]	$\Delta E^{\ddagger}_{VB}(1)$ [c]	$\Delta E^{\ddagger}_{VB}(9)$ [d]
19. X=Y=H	8.83	0.00	10.32	10.32
20. X=Cl, Y=H	4.86	0.71	10.60	10.60
21. X=Br, Y=H	14.64	14.55	16.83	17.37
22. X=I, Y=H	26.55	26.25	22.09	23.99
23. X=CH_3, Y=CH_3	16.73	0.00	14.43	14.43
24. X=SiH_3, Y=SiH_3	8.37	0.00	9.10	9.10
25. X=GeH_3, Y=GeH_3	5.76	0.00	8.34	8.34
26. X=SnH_3, Y=SnH_3	4.15	0.00	7.52	7.52
27. X=PbH_3, Y=PbH_3	1.82	0.00	6.63	6.63
28. X=CH_3, Y=SiH_3	21.73	13.06	18.29	18.72
29. X=CH_3, Y=GeH_3	26.16	20.42	21.59	22.67
30. X=CH_3, Y=SnH_3	32.85	29.06	25.50	27.79
31. X=CH_3, Y=PbH_3	40.52	38.22	29.64	33.81
32. X=SiH_3, Y=GeH_3	11.34	7.36	12.40	12.56
33. X=SiH_3, Y=SnH_3	16.99	16.00	16.31	17.09
34. X=SiH_3, Y=PbH_3	25.08	25.16	20.45	22.48
35. X=GeH_3, Y=SnH_3	10.26	8.64	12.25	12.49
36. X=GeH_3, Y=PbH_3	17.64	17.80	16.39	17.46
37. X=SnH_3, Y=PbH_3	8.29	9.16	11.66	11.96
38. X=F, Y=F	13.85	0.00	13.51	13.51
39. X=Cl, Y=Cl	5.52	0.00	10.25	10.25
40. X=Br, Y=Br	2.39	0.00	8.87	8.87
41. X=OH, Y=OH	8.20	0.00	11.70	11.70
42. X=SH, Y=SH	4.95	0.00	8.95	8.95
43. X=NH_2, Y=NH_2	11.04	0.00	10.58	10.58
44. X=C_2H, Y=C_2H	9.60	0.00	13.34	13.34
45.X=CH_2CN, Y=CH_2CN	17.62	0.00	16.02	16.02

[a] $\Delta E^{\ddagger}_{calc}$ used for VB modeling are $\Delta E^{\ddagger}$(CBS) values with ZPE correction where frequency calculation is done using cc-pVDZ basis set. [b] ΔE_{rp}=$BDE_{H\text{-}Y}$-$BDE_{H\text{-}X}$.
[c] $\Delta E^{\ddagger}_{VB}(1) = 0.3G_0 + 0.5\Delta E_{rp}$ - B; B = 0.25($BDE_{H\text{-}Y}$ + $BDE_{H\text{-}X}$).
[d] $\Delta E^{\ddagger}_{VB}(9) = \Delta E^{\ddagger}_{VB}(1) + 0.5(\Delta E_{rp})^2/G_0$.

The correlation between VB barriers ($\Delta E^{\ddagger}_{VB}$) and calculated barriers ($\Delta E^{\ddagger}_{calc}$).

Here are a few plots of the estimated VB barriers vs. CCSD(T)/CBS and DFT barriers taken from Tables S4 and S5. These can serve for the purpose of self-tutoring exercise.

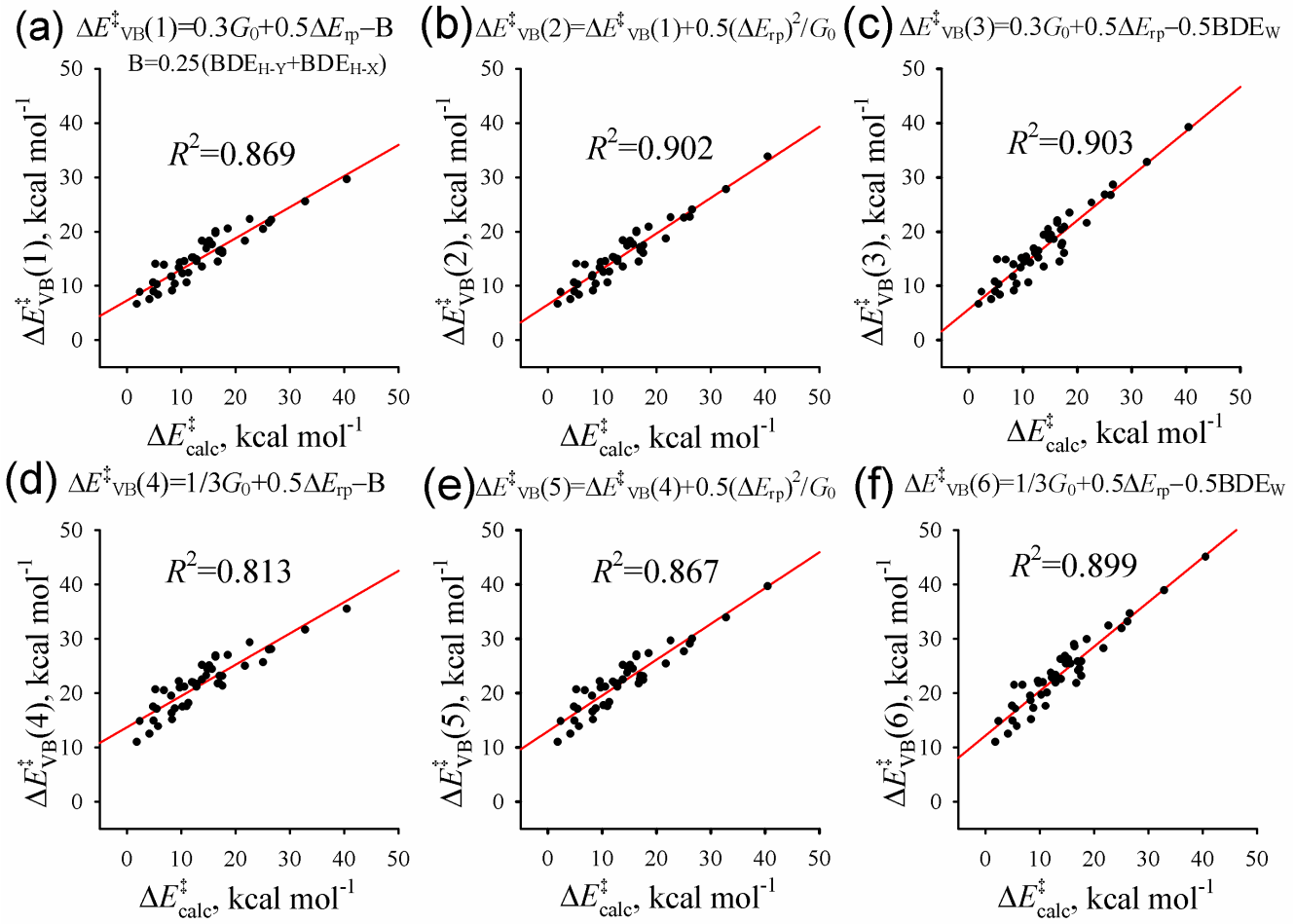

Figure S2. VB barriers plotted against calculated barriers for 45 reactions (**1-45**) using f =0.3 (a-c) and f =1/3 (d-f).

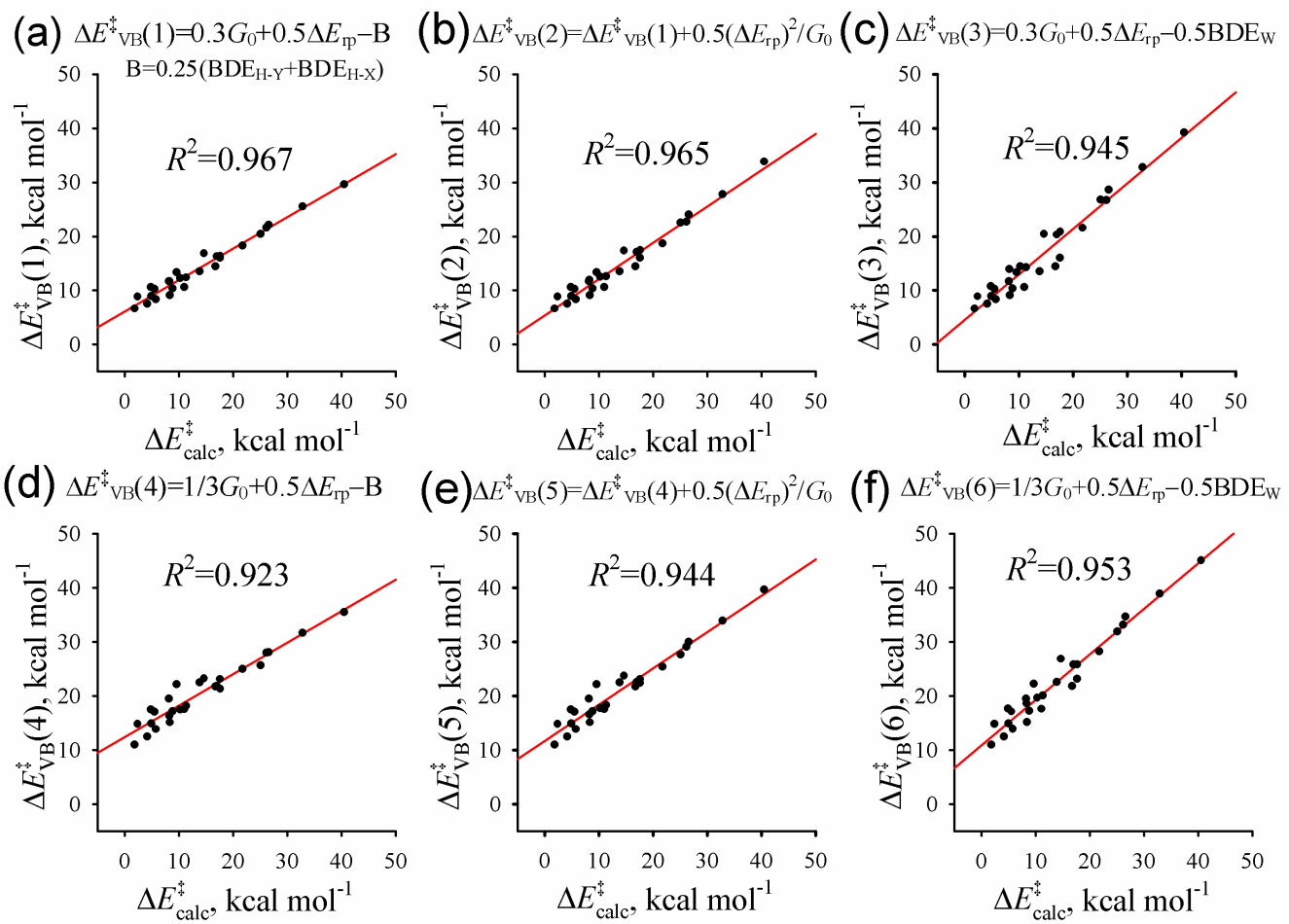

Figure S3. VB barriers plotted against calculated barriers for reactions (**19**-**45**) using f =0.3 (a-c) and f =1/3 (d-f).

Part II (b) Open and closed Shell abstractors of nonidentity reactions

This introduction is meant to assist self-tutoring in the specific topic. The VB treatment of nonidentity reactions, $X^{\bullet} + H\text{-}Y \rightarrow X\text{-}H + {}^{\bullet}Y$, requires two sets of *BDE (D)* values. When the abstractor is a closed-shell molecule, an additional promotion energy quantity (ΔE_p) is required to account for the cost of creating a radical at the abstractor site. This latter quantity simply adds to the promotion energy gap, and it can be estimated from the singlet-triplet excitation energy, e.g., of the Cr=O bond or of the α-methylstyrene. The barrier expression is related to eq. S.4, with omission of the small quadratic term, and addition of the excess promotion energy of the closed shell abstractor (X). This term appears in brackets in eq. S.5a. Equation S.5a is written explicitly in the form of eq. S.4. After using the relationship between *D*, *BDE* and *RE*, we get eq. S.5b, which is an analog of eq. S.6 for the identity barrier:

$$\Delta E_{VB}^{\ddagger} = 0.3(D_{HY} + D_{XH}) + \tfrac{1}{2}(BDE_{H\text{-}Y} - BDE_{X\text{-}H}) + \tfrac{1}{2}(BDE_{H\text{-}Y} - BDE_{X\text{-}H})^2/(D_{HY} + D_{XH}) - \tfrac{1}{4}[BDE_{H\text{-}Y} + BDE_{X\text{-}H}] \quad \text{(S.4)}$$

$$\Delta E_{VB,XY}(1)^{\ddagger} = 0.3(D_{HY} + [\tfrac{1}{2}(\Delta E_p(X)] + D_{XH}) + \tfrac{1}{2}(BDE_{H\text{-}Y} - BDE_{X\text{-}H}) - \tfrac{1}{4}[BDE_{HX} + BDE_{YH}];$$

$$\tfrac{1}{2}\Delta E_p(X) = 3/8[\Delta E_{ST}(X)] \quad \text{(S.5a)}$$

$$\Delta E_{VB,XY}(1)^{\ddagger} = 0.55BDE_{H\text{-}Y} - 0.45BDE_{H\text{-}X} + 0.3(RE_X\bullet + [\tfrac{1}{2}(\Delta E_p(X)] + RE_Y\bullet) \quad \text{(S.5b)}$$

$$\Delta E_{VB,XX}^{\ddagger} = 0.6D_{H\text{-}X} - \tfrac{1}{2} BDE_{H\text{-}X} \quad \text{(S.6)}$$

Equation S.5b shows again that the barrier will be dominated by the reorganization energy terms, which in the case of the closed-shell abstractor include the addition promotion energy term needed to create a radical center at the abstractor. Of course, the reactivity of closed-shell abstractors can be

tempered also by the thermodynamic driving force of the reaction, since the bond that is formed during the H-abstraction, e.g., •CrO-H will be weakened by the reorganization energy cost of creating a radical at the oxo center. This effect is embedded in the $BDE_{H\text{-}X}$ term in eq. S.5. To encourage you to apply the equation, we collected all the requisite data (Tables S6; see also Ref.17), while here we discussed global behavior and a few specific cases.

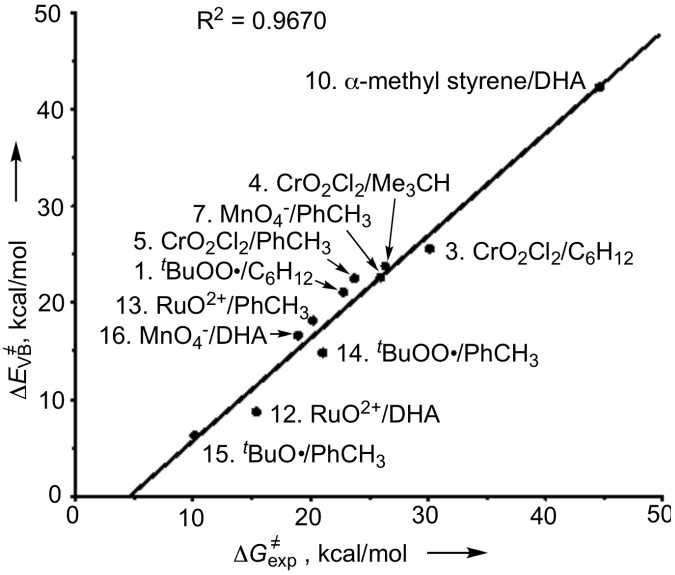

Figure S4. Plots of the VB barriers, $\Delta E_{VB,XY}(1)^{\ddagger}$ in eq. S.4, against the experimental free energies of activation, $\Delta G_{exp}^{\ddagger}$, for 11 X/Y pairs.

Figure S4 plots the estimated VB barriers based on equation 17 and using DFT computed quantities (*BDE*, *D*), against experimental $\Delta G^{\ddagger}_{exp}$ at 298K for 11 reactions. The reactant pairs X/H-Y are drawn in the Figure and one can see there a few reactions with oxyl radical abstractors $X^{\bullet}$ (reaction numbers 1,12-14 and 15), and others where the abstractor is a closed-shell molecule or ion, like CrO_2Cl_2, MnO_4^-, and α-methylstyrene (reactions 3-5, 7, 16, and 10). The correlation is seen to be reasonably good. Generally speaking, the trends in the VB barriers in Figure S4 and in the entire set of 16 reactions we tested are similar to the experimental free energies of activation.

A general observation from Figure S4 is that the reactions where the abstractor is an oxyl radical (reactions 1, 12-14 and 15 in Figure S4) have smaller VB and experimental barriers compared with those reactions where the abstractor is closed-shell (3-5,7,10 and 16). To reproduce the plot the requisite data is presented below.

Table S6. The calculated BDE, RE, *D* and ΔE_{ST} values for closed and open-shell abstractors

H-Y	LACV3P++** [a]			
	BDE	RE	*D*	ΔE_{ST}
C_6H_{12}	93.6	7.3	100.9	
Me_3CH	90.1	7.6	97.7	
$PhCH_3$ (toluene)	85.3	12.5	97.8	
camphor	93.5	7.1	101.6	
Cumyl•	45.9	32.7	78.6	74.7
α-methyl styrene)				
DHA (9,10-dihydroanthracene)	72.7	15.5	88.2	
cumene	80.8	17.6	98.4	
^tBuOO-H	77.4	7.6	85.0	
^tBuO-H	99.9	1.5	101.4	
CrO_2Cl_2H	82.4	12.8	95.2	45.4[b]
MnO_4H^-	81.0	14.8	95.8	35.5[b]
$RuOH^{2+}$	85.2	8.1	93.3	

[a]DFT calculated at B3LYP/B1(LACV3P++**). [b]The basis set used here is def2-TZVP//def2-TZVP.

Table S7. VBSCD parameters, barriers, and intrinsic barriers (kcalmol^{-1}) for nonidentity H-abstractions X + H-Y→ X-H + Y (X: a radical X• or a closed shell molecule X**:**)

Entry	X/ H-Y	G_r[a]	G_p[a]	G_0[a]	ΔE_{rp}[a]	B[a]	$\Delta E^{\ddagger}_{VB}$[b]	$\Delta G^{\ddagger}_{expt}$
1	^tBuOO•/C_6H_{12}	201.8	170.0	185.9	16.2	42.8	21.1	22.8[c]
3	CrO_2Cl_2/C_6H_{12}	235.6	190.4	213.0	11.2	44.0	25.5	30.2[c]
4	CrO_2Cl_2/Me_3CH	229.2	190.4	209.8	7.7	43.1	23.7	26.4[c]
5	$CrO_2Cl_2/PhCH_3$	229.4	190.4	209.9	2.9	43.2	22.5	23.8[c]
7	$MnO_4^-/PhCH_3$	222.2	191.6	206.9	4.3	41.6	22.6	26[c]
10	α-methyl styrene/DHA	232.5	157.2	194.9	26.8	29.7	42.2	44.7
12	RuO^{2+}/DHA	176.5	186.6	181.5	-12.5	39.5	8.7	15.4[c]
13	$RuO^{2+}/PhCH_3$	195.6	186.6	191.1	0.1	42.6	14.8	21.1[c]
14	^tBuOO•/$PhCH_3$	195.6	170.0	182.8	7.9	40.7	18.1	20.2[c]
15	^tBuO•/$PhCH_3$	195.6	202.8	199.2	-14.6	46.3	6.2	10.2[c]
16	MnO_4^-/DHA	203.1	191.6	197.3	-8.3	38.4	16.6	19.0[c]

[a]These values correspond to B1 data [LACV3P++**(6-311++G**)] given in Table S7. [b]The $\Delta E^{\ddagger}_{VB}$ values obtained using eqs. S.5a or S.5b. [c]All data are taken from the ESI of *Angew. Chem. Int. Ed*. **2012**, *51*, 5556 (ref 17 in the text).

Part III The Predictive ability of the VB Approach vs. that of the FMO approach:

As pointed out to us by a reviewer, the reader of this tutorial would want to know why should he abandon the FMO approach, in favor of the VB approach that is described in the text. Let me only say that the advantage of using our VB approach is that it covers everything that the FMO approach does, and it adds many possibilities that are beyond the FMO capabilities. Nevertheless, since the reviewer requested to point out specific areas where FMO does not work while VB works, we are listing here a sample of problems of the many we know:

(a) At a general level, the VB approach shows the origins of the barrier and the TS, and the emergence of stepwise mechanisms. As the text shows it allows also predicting barriers from raw data. FMO theory can do none of these. In fact most of the material covered in the tutorial is beyond FMO.

(b) The FMO approach cannot be used unambiguously for making predictions on odd electron systems, such as radical reactions, reactions of radical cations and radical anions, etc. In all of these cases the FMO user has to make a prediction, which of two orbital interactions, e.g., SOMO-HOMO or SOMO-LUMO, is more important. This cannot be done with much certitude. As such, FMO theory will not be able to make clear predictions about stereoselectivity and regioselectivity of odd-electron reactions. The VB method is very good at that, and is the only qualitative approach that can make such predictions. The interested reader may look at the additional references in Section 4 of the References above (**Predictions of stereoselectivity and regioselectivity using VB theory**). Many other examples can be found in Refs. 14 and 29 of the text.

(c) The VB approach makes predictions about isoelectronic species that change character from transition states to stable intermediates, e.g., H_3 vs. Li_3 (also H_4 vs. Li_4, H_6 vs. Li_6), H_3^- vs. X_3^- (X = halogen), CL_5^- vs. SiL_5^- (see e.g., Refs. 14 and 29 of the text). The FMO approach is not applicable to these questions.